

Power Quality Enhancement Strategy In Grid Connected Dual Voltage Source Inverters Supplying Various Loads

Abinash Kshatri^{1*}, Sandeep Dhama¹, Amrit Bhatta¹

¹Department of Electrical Engineering, Pashchimanchal Campus, Pokhara
IOE, Tribhuvan University, Nepal

*abinashkshatri123@gmail.com

(Manuscript Received 1st September, 2024; Revised 24th September, 2024; Accepted 28th October, 2024)

Abstract

This paper presents power quality improvement technique for grid connected dual inverter systems supplying non-linear and unbalanced loads. Control algorithms based on instantaneous symmetrical component theory (ISCT) are implemented in the dual voltage source inverter(DVSI). The DVSI enhance power quality by injecting real power and compensating for reactive, harmonic, and nonlinear loads. The dq0 transformation technique is utilized for effective voltage analysis at the Point of Common Coupling (PCC). Detailed simulation results validate the control strategy, demonstrating significant reduction in Total Harmonic Distortion(THD) and improved power quality. THD is analyzed for nonlinear and unbalanced load and reduced below 3%. The findings indicate that the DVSI scheme effectively mitigates harmonic problems, ensuring stable and reliable operation of interconnected grids, and complies with IEEE standards for THD and frequency maintenance.

Keywords- Harmonics, Inverter, Nonlinear Loads, Power Quality

1. Introduction

The technologies developed in response to environmental concerns created the currently existing conventional power infrastructure. An inverter connected to the grid permits power flow; it transfers energy generated in the microgrid to the main grid and associated loads. The power quality should be maintained with the grid connection of a microgrid; especially, since it uses an increased number of power electronic devices, electrical nonlinear loads, and unbalances that are produced by those loads. Surely, this affects power quality. The key power quality problem is supplying harmonic distortions which also guarantee optimal systems performance, stability, and reliability of the grids interconnected.

The paper tends to aim at the analysis of THD in microgrids owing to nonlinear loads at the grid, point of common coupling (PCC), and load side before and after the installation of the DVSI system and conclude how the DVSI mitigates the harmonic problem from the system using this scheme. The paper discusses

a new idea of dual voltage source inverter that caters to work in conjunction with microgrid systems. One main voltage source inverter injects the real power generated by a microgrid to the utility grid, while another additional voltage source inverter works on reactive power, harmonics, and unbalanced load-related issues. Thus, the rated capacity of MVSI is optimally exploited for injecting power in case there is a surplus of renewable energy generation. This is easily done by making these two inverters act to distribute a load power; hence, power losses across semiconductor switches are minimized. It is better reliable compared to a single multifunctional inverter. Smaller modular inverters operating at higher switching frequencies reduce the size and cost of filters and interfacing inductors (Kumar et al., 2015), (Zhang et al., 2013), (Kahrobaeian & Mohamed, 2012).

The dq0 transformation technique is employed for extracting the fundamental positive sequence of the PCC voltage. This may be looked upon as a method for filtering out

only the desired component selectively from the total voltage signal for further analysis. Once the signal has undergone dq0 transformation, it is easy for the control system to have only the fundamental positive sequence of the PCC voltage concentrated upon. As a result, this will make sure that the DVSI scheme operates accurately and efficiently. The performance of the control strategy was validated through a detailed simulation and experimental results (Iyer et al., 2005), (Tummuru et al., 2014).

The result is energy losses, mainly due to the harmonic distortions, poor voltage regulation, and reduction in the power factor, with nonlinear loads, for instance, power electronic equipment; hence the PQ problems. The various control strategies implemented for PQ include the use of passive compensators, namely, LC filters. Not all harmonic distortions, however, can be treated with LC filters alone; hence, other methods become imperative, amongst which is quite efficient the dual voltage source inverter method for improving power quality. The work will, therefore, be channeled towards finding the control strategy for DVSI that yields improved power quality for a grid-connected microgrid through mitigation of harmonic distortions due to nonlinear loads. Some specific aims are voltage regulation at the PCC, attenuation of harmonic distortions, and making the grid current balanced and sinusoidal. Specific advantages of DVSI include higher reliability, cost-effectiveness due to reduced filter size, and effective use of inverter capacity, where the main inverter feeds the active power while the auxiliary inverter compensates the reactive and harmonic loads (Kumar et al., 2015), (Kahrobaeian & Mohamed, 2012), (Guerrero et al., 2013).

2. System Related Theories and Concept

2.1. Dual Voltage Source Inverter

To explain concept of DVSI, consider a power system with a grid on one terminal and nonlinear loads on the other terminal. Here the

system includes a three-level NPC inverter for the realization of AVSI and a three-legged inverter for the MVSI, which are all connected at the Point of Common Coupling (PCC) in order to feed the power into the loads. As seen from fig 1 below, $i_{g(abc)}$, $i_{ugm(abc)}$, and $i_{ugx(abc)}$ are grid currents, MVSI currents, and AVSI currents in three phases, respectively. The three-phase load currents are represented as i_{labc} . The AVSI employs a DC link implemented as split capacitor configuration with two capacitors, C_1 and C_2 , both rated at $2000 \mu F$ (Kumar et al., 2015), (Iyer et al., 2005), (Singh et al., 2011).

The scheme injects real power from the DERs into an electrical grid through an MVSI, using a filter inductance L_{fm} and resistance R_{fm} , that assist in oscillations' damping in the injected current. The DER either can be coupled to the DC link by a DC Source or an AC source interfaced through a rectifier. The compensating function for reactive power, harmonic currents, and imbalanced loads by the auxiliary inverter uses its own filter inductance L_{fx} and resistance R_{fx} . The required switching pulses are generated for these two inverters in accordance with the computed reference currents: $i_{ugm(abc)}^*$ and $i_{ugx(abc)}^*$ for the main and secondary, respectively (Zhang et al., 2013), (Guerrero et al., 2013).

The control and computation module is one of the most important modules for the operation of the workings of the DVSI system. In the case of calculating the primary inverter reference current, $V_{t(abc)}$ appears while, at the same time, it is used in the calculation of the auxiliary inverter reference current. Instantaneous active power calculation and low-pass filter: The active power is calculated from the load current $i_{l(abc)}$ and filtered into a low-pass filter to smooth the controls. abc components are converted into $dq0$ components with the help of the $dq0$ transformation and sequence analyzer for better analysis and control, after which they are inversely converted back to abc after filtering. A PI controller of DC link voltage V_{dc} maintains the reference value V_{dcref} is $1040V$.

Harmonics are present at the PCC due to the existence of unbalanced and nonlinear loads where grid, load, and inverters meet. It samples the voltage at the PCC, $V_{l(abc)}$, along with the load current, $i_{l(abc)}$; the abc measurements are then converted into $dq0$ components for ease of analysis and effective control. For this, reference currents are estimated with respect to both the main and auxiliary inverters, in which the former injects the real power and the latter compensates the power in terms of reactive, harmonics, and unbalances. PWM generates switching pulses to control the output of inverters.

2.2 Instantaneous Symmetrical Component Theory

ISCT was developed primarily for unbalanced and nonlinear load compensations by active power filters. The system topology shown in Fig.1 is used for realizing the reference current for the compensator. The ISCT for load compensation is derived based on the following three conditions (Tummuru et al., 2014).

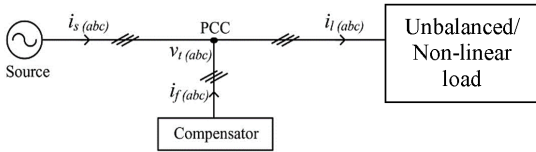


Fig. 1: Schematic of a Compensator

The source neutral current must be zero. Therefore

$$i_{sa} + i_{sb} + i_{sc} = 0 \quad (1)$$

The phase angle between the fundamental positive sequence () voltage and source current is (i_{sa}) is ϕ

$$\angle v_{ta}^+ = \angle i_{sa} + \phi \quad (2)$$

The average real power of the load (PL) should be supplied by the source

$$v_{ta1}^+ i_{sa} + v_{tb1}^+ i_{sb} + v_{tc1}^+ i_{sc} = P_L \quad (3)$$

Solving the above three equations, the reference source currents for 3 phase can be obtained as:

$$i_{s(abc)}^* = \left(\frac{v_{t(abc)1}^+}{\sum_{j=a,b,c} v_{tj}^{+2}} \right) P_L \quad (4)$$

Where $i_s^*(a)$, $i_s^*(b)$, $i_s^*(c)$ positive sequence of load currents drawn from source ,when it supplying an average load power P_L . The power (PL) can be calculated using a moving average filter, employing a window of one-cycle data points, as described below-

$$P_L = \int_{t_1-T}^{t_1} (v_{ta1}^+ i_{sa} + v_{tb1}^+ i_{sb} + v_{tc1}^+ i_{sc}) dt \quad (5)$$

where, t_1 is any arbitrary time instant

Finally, the reference currents for the compensator can be generated as follows:

$$i_{f(abc)}^* = i_{l(abc)} - i_{s(abc)}^* \quad (6)$$

Equation (6) can be used to generate the reference filter currents using ISCT, when the entire load active power, PL is supplied by the source and load compensation is performed by a single inverter. A modification in the control algorithm is required, when it is used for DVSI scheme. The following section discusses the formulation of control algorithm for DVSI scheme. The source currents, $i_{s(abc)}$ and filter currents $i_{f(abc)}$ will be equivalently represented as grid currents $i_{gl(abc)}$ and AVSI currents $i_{\mu gx(abc)}$, respectively, in further sections.

2.3 abc – $\alpha\beta$ –dq transformation

Clarke Transformation: The Clarke transformation is used to convert three-phase quantities (abc) into two-phase stationary quantities ($\alpha\beta$).

The Park transformation: It is also known as the $dq0$ transformation and is used to transform the two-phase stationary quantities ($\alpha\beta$) into two-phase rotating quantities (dq).

The Clarke transform uses three-phase currents i_a , i_b and i_c to calculate currents in the two-phase orthogonal stator axis: i_α and i_β . These two currents in the fixed coordinate stator phase are transformed to the i_{sd} and i_{sq} currents components in the dq frame with the Park transform .The PCC voltages in natural reference frame (v_{ia} , v_{ib} , and v_{ic}) are first

transformed into $dq0$ reference frame as given by:

$$\begin{bmatrix} v_{td} \\ v_{tq} \\ v_{t0} \end{bmatrix} = C \begin{bmatrix} v_{ta} \\ v_{tb} \\ v_{tc} \end{bmatrix}. \quad (7)$$

Where,

$$C = \sqrt{\frac{2}{3}} \begin{bmatrix} \sin \theta & \sin(\theta - \frac{2\pi}{3}) & \sin(\theta + \frac{2\pi}{3}) \\ \cos \theta & \cos(\theta - \frac{2\pi}{3}) & \cos(\theta + \frac{2\pi}{3}) \\ \frac{1}{\sqrt{2}} & \frac{1}{\sqrt{2}} & \frac{1}{\sqrt{2}} \end{bmatrix} \quad (8)$$

Transformed voltages in $dq0$ frame (v_{td} and v_{tq}) contain average and oscillating components of voltages. These can be represented as

$$v_{td} = \bar{v}_{td} + \tilde{v}_{td} \quad (9)$$

$$v_{tq} = \bar{v}_{tq} + \tilde{v}_{tq} \quad (10)$$

Where, $\bar{\cdot}$ represent the average components. $\tilde{\cdot}$ indicate the oscillating components of v_{td} and v_{tq} respectively. These dq components are again converted into three phase quantities (abc) (Schonardie et al., 2012).

2.4 Moving average filter

A moving average filter is a simple and commonly used method for smoothing time-series data or reducing noise in signals. It is a type of low-pass filter that works by averaging values within a moving window of a specified size. The moving average helps to highlight the underlying trends in the data by smoothing out short-term fluctuations or random noise. The output of the moving average filter is the sequence of averaged values.

Moving Average Filter filters out the oscillating components of the transformed voltages in $dq0$ frame leaving only the average component behind. Hence, the equation becomes (Golestan et al., 2014):

$$v_{td} = \bar{v}_{td} \quad (11)$$

$$v_{tq} = \bar{v}_{tq} \quad (12)$$

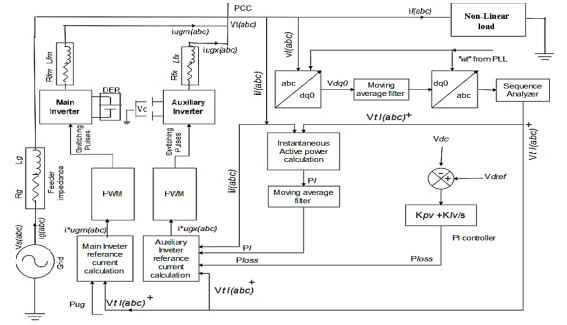


Figure 2: Schematic diagram showing the control strategy of a DVSI scheme

2.5 Sequence Analyzer

The Sequence Analyzer block takes a three-phase signal (usually voltage) as the input and outputs the magnitude and phase of the positive, negative, or zero sequence. The input signals are first converted to phasor representation based on the base frequency and harmonic specified in the block mask. The block then transforms the phasor into a sequence of components. A positive sequence analyzer is often used in the context of power systems analysis, particularly in three-phase systems. The positive sequence refers to the part of the signal or system that rotates in the same direction as the original phasors. Positive sequence analysis is important in power system stability studies and fault analysis. One common technique to extract the positive sequence components from three-phase quantities is to use the Clarke transformation followed by a filtering process. For positive sequence of PCC voltages (Kumar et al., 2015), (Singh et al., 2011):

$$\begin{bmatrix} v_{ta}^+ \\ v_{tb}^+ \\ v_{tc}^+ \end{bmatrix} = C^T \begin{bmatrix} \bar{v}_{td} \\ \bar{v}_{tq} \\ 0 \end{bmatrix} \quad (13)$$

3. Control Methodology

3.1 MVSI Control Strategy and Reference Current Generation

The DC-link voltage of the MVSI is established at $650V$. Employing an LR filter

with an inductance (L_{fm}) of 5mH and resistance (R_{fm}) of 0.25Ω , the MVSI delivers a balanced sinusoidal current with a unity power factor. This results in the absence of zero sequence switching harmonics in the MVSI output current, reducing the filter requirements in comparison to AVSI. The MVSI controller generates gate signals, utilized for switching the MVSI inverter as depicted in the figure. VI measurements are conducted to gauge the inverter's output voltage and current. The output is connected to the main grid using an RL filter. Now the MVSI reference currents can be obtained as:

$$i_{\mu gm}^* = \left(\frac{v_{t(abc)1}^+}{\sum_{j=a,b,c} v_{tj}^{+2}} \right) P_{\mu g} \quad (14)$$

Where, $P_{\mu\sigma}$ is the available power at the dc link

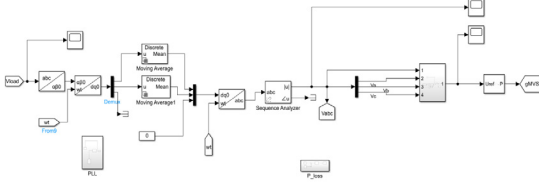


Fig. 3: Controller for MVSI

3.2 AVSI Control Strategy and Reference Current Generation

The crucial elements of AVSI are DC storage capacitors (C_1 and C_2), and interfacing inductance (L_{fx}). The DC-link voltage across each capacitor is set at 1.6 times the peak of the phase voltage. The total DC-link voltage reference (V_{dcref}) is identified as $1040V$, with the values of C_1 and C_2 chosen as $2000\mu F$ each. The interfacing inductance (L_{fx}) is specified as 20mH, and the corresponding resistance (R_{fx}) is 0.25Ω . The gate signal from the AVSI controller is employed for switching the AVSI inverter, as illustrated in the figure. VI measurements are conducted to assess the inverter's output voltage and current. The output is linked to the Point of Common Coupling (PCC) through the use of an RL filter (Iyer et al., 2005).

The auxiliary inverter requires a constant dc-link voltage for proper operation. Variations in the dc-link voltage are caused by switching and ohmic losses, termed as P_{loss} and

compensated by the grid. A PI controller is used to generate $P_{i, \dots}$ term as given by

$$P_{Loss} = K_{pv} e_{vdc} + K_{iv} \int e_{vdc} dt \quad (15)$$

Where, $e_{vdc} = V_{dcref} - V_{dc}$, K_{pv} and K_{iv} are dc voltage controller gains whose values are 10 and 0.05 respectively. V_{dc} represents actual voltage sensed and updated once in a cycle. AVSI reference currents can be obtained as given

$$i_{\mu gn}^* = i_{ln} - \left(\frac{v_{t(n)1}^+}{\sum_{j=a,b,c} v_{tj}^{+2}} \right) (P_L + P_{Loss}) \quad (16)$$

Where, $n = a, b \& c$

Applying the KCL at PCC from fig.1, we get the reference grid current which is given by

$$i_{ga}^* = \left(\frac{v_{t(a)1}^+}{\sum_{j=a,b,c} v_{tj}^{+2}} \right) (P_L + P_{Loss} - P_{\mu g}) \quad (17)$$

The above equations are used to model reference current generation block for AVSI as shown in figure 4.

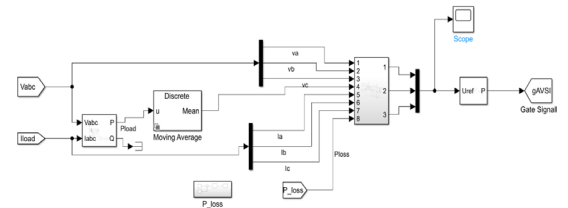


Fig. 4: Controller for AVSI

3.3 Overall System Modeling

The complete system comprising of grid connected DVSI, controllers and loads is modelled in matlab. The parameters used for modelling is presented in Table 1. The overall system model is shown in figure 5.

Table 1: System Parameter for Simulation Study

Parameters	Values
Grid voltage	400 V (L-L)
Frequency	50 Hz
AVSI	$L_{fx}=20$ mH , $R_{fx} =0.25\Omega$
MVSI	$L_{fx}=5$ mH , $R_{fx} =0.25\Omega$ & dc link voltage =650 V
Nonlinear load	3 Φ diode bridge rectifier with DC side current of 3A
PI controller's Gains	$K_{pv} =10$ & $K_{iv} = 0.05$

4. Result and Discussion

The DVSI supplying non-linear load is simulated in MATLAB with and without ICT control strategy. Load is varied at 0.3 and 0.4 seconds by adding linear unbalanced load to analyze frequency variation. THD is also analyzed by using FFT tool in MATLAB software. Voltage and current waveforms, frequency waveform and harmonics distortions are analyzed for various loads.

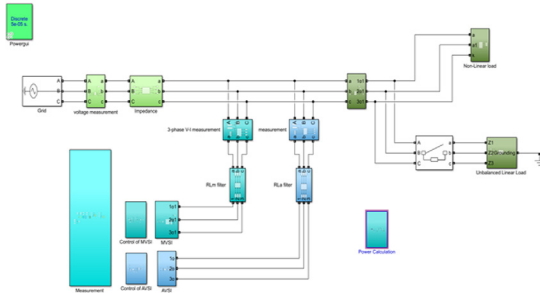


Fig. 5: Overall System Diagram

4.1 Voltage Waveforms and THD at PCC

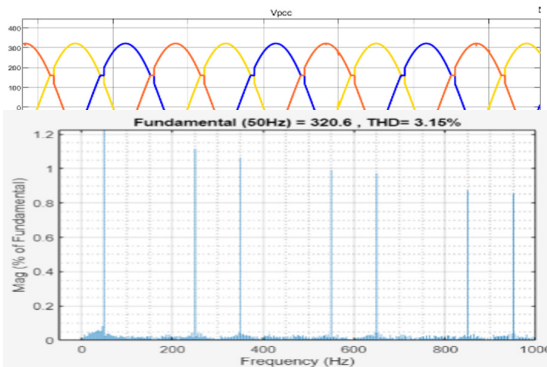


Fig. 6a. Voltage at PCC without DVSI

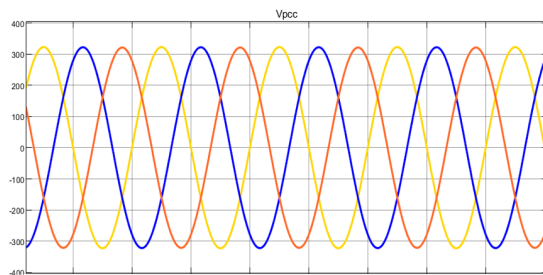


Fig. 6b. THD of Voltage at PCC without DVSI

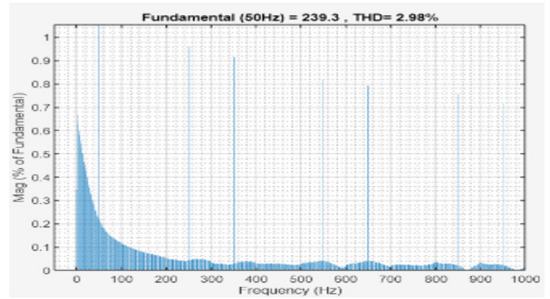
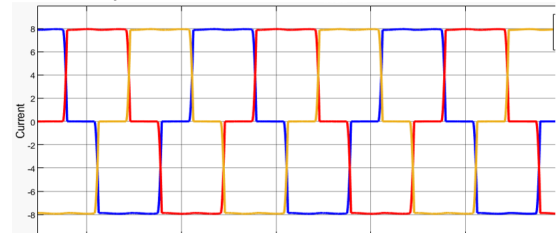


Fig. 7a. Voltage at PCC with DVSI

Fig. 7b. THD of voltage at PCC with DVSI

Figure 6 represents the voltage analysis of the system at the PCC before and after the installation of a DVSI. Without DVSI, the voltage waveform at the PCC is distorted as in Figure 6a. The corresponding THD spectrum depicted in Figure 6b is 3.16% showing a high harmonic content in the voltage. Once the DVSI is installed as per Figure 7a, the voltage waveform at the PCC became regular and less distorted. This is further confirmed by the THD spectrum in Figure 7b showing a THD of 2.98%. The reduced value of THD signifies the improvement in power quality because of the fact that a DVSI ensures better mitigation of harmonics and better performance of the overall system.



4.2 Current Waveform and THD

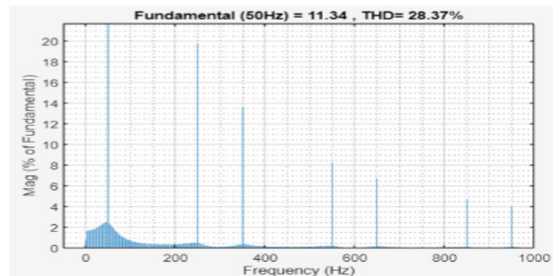


Fig. 8a: Current Drawn by Nonlinear Load

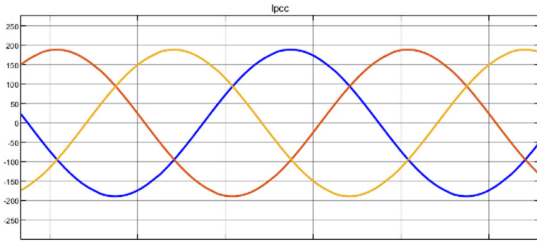


Fig. 8b THD of Current at PCC without DVSI

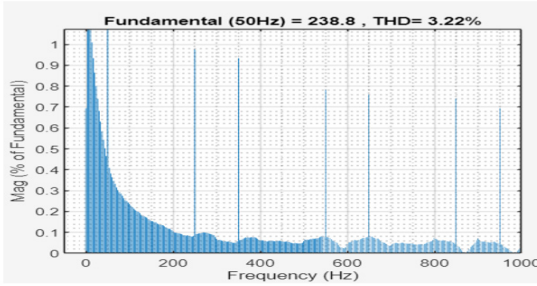


Fig. 9a. Grid Current at PCC with DVSI

Fig. 9b. THD of Current at PCC with DVSI

The figure 8a shows the current drawn by non-linear load. Non-linear load causes highly distorted current waveform in the PCC, indicating a huge harmonic content. The THD spectrum about this is shown in Figure 8b, which is very high at 28.37%, depicting substantial harmonics in the current.

Indeed, Figure 9a highlights that, after the implementation of the DVSI, the current waveform at the PCC becomes much smoother and more sinusoidal since most of the distortions were eliminated. Such improvement is confirmed also by the THD spectrum shown in Figure 9b, where it appears that the total harmonic distortion drastically drops to 3.22%. This large reduction of THD could be proof of the efficiency of the DVSI in mitigating harmonics. Therefore, good quality current became possible, based on which the performance of the overall system was also improved.

4.3 Frequency Waveform

Figure 10 depicts the grid frequency stability, MVSI, AVSI, and load versus load fluctuations caused by adding linear unbalanced loads. In fact, $Z_1 = 35 + j19 \Omega$, $Z_2 = 30 + j15 \Omega$, and $Z_3 = 23 + j12 \Omega$ were added to the circuit. These loads were added within the

time of $t_1 = 0.3$ seconds and $t_2 = 0.4$ seconds, within which time the frequency across these components was observed. The overall system frequency remained between 50 ± 0.5 Hz, even with noticeable fluctuations in the MVSI, AVSI, and especially in the load. Accordingly, the frequency of the grid remained mostly stable and the overall frequency stability was well maintained by the DVSI system, meaning this kind of unbalanced change in loads did not badly affect the continuity of the operation. The frequency of different parameter overlaps that's why it seems two graph but there is overall system and there compression in single graph.

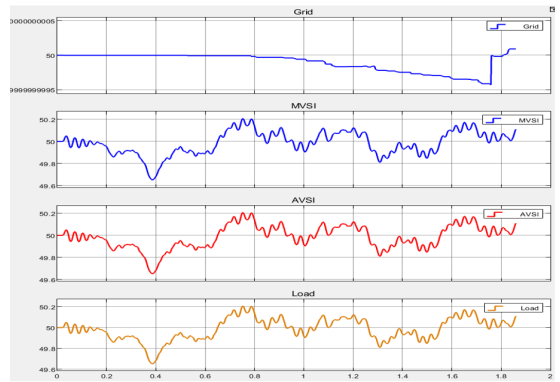


Fig. 10. Frequency of Grid , MVSI, AVSI, Load Respectively During Fluctuation of Load

5. Conclusion

The power system has evolved with technological development and consideration for the environment to increase in the use of renewable energy sources, especially in microgrids. For the improvement of power quality in such an environment, a DVSI is used. The two halves of the DVSI are a real-power-injecting Main Voltage Source Inverter and an compensating (reactive power, harmonics, and unbalanced loads) Auxiliary Voltage Source Inverter. With this approach, inverter capacity utilization can be optimized with greater system reliability at lower DC grid voltage ratings and smaller filter size.

The operation of the DVSI in a grid-

connected mode is controlled through control algorithms based on ISCT, which try to mitigate power quality problems like voltage regulation, harmonic distortion limitation, and balanced grid currents. MATLAB modeling justify that active power to the load is supplied mainly by the MVSI, while reactive power compensation, harmonics, and unbalanced conditions are compensated by the AVSI. The system uses a moving average filter to wipe off the oscillating components and a sequence analyzer for finding the positive sequence voltage for reference current calculation. This will ensure accurate and effective mitigation in power quality.

The results show, through simulation, the effectiveness of the DVSI scheme in microgrid applications. The results have proven that this scheme follows the IEEE standards with regard to the THD and regulation of frequency, hence always keeping the THD below 5% (overall) The frequency is also always within the standard value of 50 Hz, further verifying the viability of the DVSI for power quality improvement in microgrid applications.

References

- Kumar, M. V., Mishra, M. K., & Kuma, C. (2015). A grid-connected dual voltage source inverter with power quality improvement features. *IEEE Transactions on Sustainable Energy*, 6(2), 482–490.
- Zhang, Y., Gatsis, N., & Giannakis, G. B. (2013). Robust energy management for microgrids with high-penetration renewables. *IEEE Transactions on Sustainable Energy*, 4(4), 944–953.
- Kahrobaeian, A., & Mohamed, Y.-R. (2012). Interactive distributed generation interface for flexible micro-grid operation in smart distribution systems. *IEEE Transactions on Sustainable Energy*, 2(3), 295–305.
- Iyer, S., Ghosh, A., & Joshi, A. (2005). Inverter topologies for DSTATCOM applications: A simulation study. *Electric Power Systems Research*, 75(23), 161–170.
- Tummuru, N. R., Mishra, M. K., & Sriniva, S. (2014). Multifunctional VSC controlled microgrid using instantaneous symmetrical. *IEEE Transactions on Sustainable Energy*, 5(1), 313–322.
- Guerrero, J., Loh, P. C., Lee, T.-L., & Chandorkar, M. (2013). Advanced control architectures for intelligent microgrids—Part II: Power quality, energy storage, and ac/dc microgrids. *IEEE Transactions on Industrial Electronics*, 60(4), 1263–1270.
- Singh, M., Khadkikar, V., Chandra, A., & Varma, R. (2011). Grid interconnection of renewable energy sources at the distribution level with power-quality improvement features. *IEEE Transactions on Power Delivery*, 26(1), 307–315.
- Schonardie, M., Coelho, R., Schweitzer, R., & Martins, D. (2012). Control of the active and reactive power using dq0 transformation in a three-phase grid-connected PV system. *IEEE Transactions on Power Electronics*, 29(6), 2750–2763.
- Golestan, S., Ramezani, M., Guerrero, J. M., Freijedo, F. D., & Monfared, M. (2014). Moving average filter-based phase-locked loops: Performance analysis and design guidelines. *IEEE Transactions on Power Electronics*, 29(6), 2750–2763.